Pseudomonas syringae differentiates into phenotypically distinct subpopulations during colonization of a plant host

José S. Rufián[1], María-Antonia Sánchez-Romero[2], Diego López-Márquez[1], Alberto P. Macho[3], John W. Mansfield[4], Dawn L. Arnold[5], Javier Ruiz-Albert[1], Josep Casadesús[2], Carmen R. Beuzón[1]*

[1]Instituto de Hortofruticultura Subtropical y Mediterránea, Universidad de Málaga-Consejo Superior de Investigaciones Científicas (IHSM-UMA-CSIC), Depto. Biología Celular, Genética y Fisiología, Campus de Teatinos, Málaga E-29071, Spain

[2]Departamento de Genética, Facultad de Ciencias, Universidad de Sevilla, Apartado 1095, 4108 Seville, Spain

[3]Current address: Shanghai Center for Plant Stress Biology, Shanghai Institutes of Biological Sciences, Chinese Academy of Sciences, Shanghai 201602, China

[4]Faculty of Natural Sciences, Imperial College, London, SW7 2AZ, United Kingdom

[5]Centre for Research in Bioscience, Faculty of Health and Applied Sciences, University of the West of England, Frenchay Campus, Bristol, BS16 1QY, United Kingdom

Running head: Formation of bacterial subpopulations in a plant host

*For correspondence: cbl@uma.es

Phone: ++ 34-952-131959

Fax: ++ 34-952-132001

Keywords: phenotypic heterogeneity, bacterial pathogen, bistability, plant host, type III secretion system, bacterial effectors, virulence, host adaptation

ABSTRACT

Bacterial microcolonies with heterogeneous sizes are formed during colonization of *Phaseolus vulgaris* by *Pseudomonas syringae*. Heterogeneous expression of structural and regulatory components of the *P. syringae* type 3 secretion system (T3SS), essential for colonization of the host apoplast and disease development, is likewise detected within the plant apoplast. T3SS expression is bistable in the homogeneous environment of nutrient-limited T3SS-inducing medium, suggesting that subpopulation formation is not a response to different environmental cues. T3SS bistability is reversible, indicating a non-genetic origin, and the $T3SS^{HIGH}$ and $T3SS^{LOW}$ subpopulations show differences in virulence. T3SS bistability requires the transcriptional activator HrpL, the double negative regulatory loop established by HrpV and HrpG, and may be enhanced through a positive feedback loop involving HrpA, the main component of the T3SS pilus. To our knowledge, this is the first example of phenotypic heterogeneity in the expression of virulence determinants during colonization of a non-mammalian host.

SIGNIFICANCE

The plant pathogen *Pseudomonas syringae* requires a type III secretion system (T3SS) to inject effector proteins into host cells and to cause disease. This study shows that expression of T3SS genes is activated in a heterogeneous fashion during colonization of plant tissues. Cell-to-cell differences in T3SS gene expression are likewise observed in the homogeneous environment of nutrient-limited culture medium, where an isogenic bacterial population bifurcates into lineages that express or not the T3SS. Differences in T3SS expression are non-heritable, are established through the action of a double-negative regulatory feedback loop, and determine differences in plant disease severity. Phenotypic heterogeneity is therefore a factor that must be considered when portraying bacterial adaptation to plant niches.

INTRODUCTION

Bacterial infections involve spatial and temporal changes in gene expression that accompany the migration of pathogens from the site of invasion to target tissues. Pathogen progression inside the host is therefore accompanied by physiological adjustments to respond to different stimuli and microenvironments. However, phenotypic changes are not always deterministic, directly correlated with stimuli. Stochastic events such as an uneven distribution of regulators during cell division can produce cell-to-cell differences within a homogeneous microenvironment. This can lead to probabilistic determination of certain phenotypic traits, generally known as phenotypic heterogeneity or phenotypic variation (Davidson and Surette, 2008).

Phenotypic heterogeneity has been known to take place in microbial clonal populations for decades (Bigger, 1944; Novick and Weiner, 1957). In certain cases, phenotypic heterogeneity merely reflects the occurrence of cell-to-cell differences generated by molecular noise. In other cases, however, phenotypic heterogeneity reflects the occurrence of bistability, the bifurcation of a unimodal physiological state into two distinct states, generating two bacterial subpopulations or lineages.

Bistability is usually the consequence of bimodal gene expression, which can be generated by a positive feedback loop as described in the *E. coli lac* operon (Novick and Weiner, 1957) or by a double negative feedback loop as in the lysis/lysogeny decision of bacteriophage lambda (Novick and Weiner, 1957; Herskowitz and Hagen, 1980). The literature on bacterial bistable switches has been enriched with interesting examples in the last decade (Dubnau and Losick, 2006; Davidson and Surette, 2008; van der Woude, 2011; Sánchez-Romero

and Casadesús, 2014; van Vliet and Ackermann, 2015; Uphoff et al., 2016). In certain cases, the biological significance of bistability remains a mystery. In other examples, however, subpopulation formation may be viewed either as a division of labour within the population or as a bet-hedging strategy that may facilitate adaptation to environmental challenges (Veening et al., 2008).

The importance of analysing phenotypic heterogeneity has been highlighted in the context of antibiotic exposure for animal and human and in the colonization of animals (Helaine and Holden, 2013; Arnoldini et al., 2014; Campbell-Valois et al., 2014; Claudi et al., 2014; Sánchez-Romero and Casadesús, 2014; Manina et al., 2015; Bram Van den Bergh, 2016; Brian P. Conlon, 2016; Victor I. Band, 2016). In *Salmonella enterica* pathogens, for instance, phenotypic heterogeneity has been observed at several stages of host colonization including invasion of the intestinal epithelium, survival in macrophages, and colonization of the gall bladder (Stecher et al., 2004; Saini et al., 2010; Bäumler et al., 2011; Stewart and Cookson, 2012). Other examples that highlight the relevance of phenotypic heterogeneity in bacterial infections are bistable expression of the cholera toxin in *Vibrio cholerae* (Nielsen et al., 2010), and of the NO-detoxification system in *Yersinia pseudotuberculosis* (Davis et al., 2015).

Despite increasing evidence supporting the notion that bacterial pathogens exploit non-genetic variation to adapt to mammalian hosts, little is known about the occurrence or potential impact of these processes in the adaptation of bacteria to non-animal hosts. In this work, we have addressed this issue in the archetypal plant pathogen *Pseudomonas syringae* (Mansfield et al., 2012). *P. syringae* is an academically relevant model pathogen of increasing economical,

impact in agriculture, with recent resurgence of old diseases and emergence of new ones (Shenge, 2007; Green et al., 2010).

P. syringae enters the plant from the leaf surface through natural openings or wounds reaching the intercellular spaces of the leaf parenchyma, the apoplast, where it replicates. In the apoplast, *P. syringae* uses a type III secretion system (T3SS) to deliver effector proteins into the plant cell cytosol (Alfano and Collmer, 1997; Rohmer et al., 2004). Many of these effectors act to suppress plant defences to allow bacterial colonization (Macho and Zipfel, 2015).

In this study, we show that phenotypic heterogeneity occurs during plant colonization by *P. syringae*. Structural and regulatory components of the *P. syringae* T3SS display heterogeneous expression within the plant apoplast, and bistable T3SS expression is detected in the homogeneous environment of nutrient-limited T3SS-inducing medium. T3SS bistability is reversible, supporting a non-genetic origin, and generates bacterial subpopulations with differences in virulence. To our knowledge, this is the first example of bacterial phenotypic heterogeneity in a non-mammalian host.

RESULTS

Expression of the T3SS is heterogeneous within the plant apoplast

Following the dynamics of fluorescently labelled *P. syringae* pv. *phaseolicola* populations during colonization of *Phaseolus vulgaris*, we observed that the size of bacterial microcolonies within the apoplast was heterogeneous (Fig. 1A and B). Since the apoplast is a complex and multifarious environment, heterogeneity might reflect adaptation of *P. syringae* to distinct microenvironments. An alternative possibility, however, is that heterogeneous colony size might result from random differences in the expression of virulence factors, as described in certain animal pathogens (Nielsen et al., 2010; Davis et al., 2015).

To evaluate if apoplast-growing bacteria could display heterogeneous gene expression, we applied single-cell methods to analyse transcriptional fusions to *gfp* of several *P. syringae* genes. Given the relevance of the T3SS in plant colonisation by *P. syringae*, we focused our study on T3SS genes. The choice was further supported by a report on the necrotrophic plant pathogen *Dickeya dadantii* showing that a plasmid-cloned type III promoter displayed phenotypic heterogeneity under laboratory conditions (Zeng et al., 2012). We generated transcriptional fusions to *gfp* downstream of chromosome-located native copies of three genes encoding T3SS elements: *hrpL*, encoding an alternative sigma factor of the extracytoplasmic factor (ECF) family (Fouts et al., 2002), *hrcU*, the promoter-distal gene of the HrpL-controlled *hrcQRSTU* operon, encoding a structural component of the T3SS (Charkowski et al., 1997), and *hopAB1*, encoding a type III secreted effector involved in suppressing plant defences (Jackson et al., 1999). All three strains displayed wild type virulence (Fig. S1). Bacterial distribution within a microcolony developing in the confines of the

intercellular spaces of the leaf apoplast is heterogeneous (Fig. S2 and Video S1 and S2) and can thus lead to apparent differences in fluorescence intensity as judged by microscopic examination. Therefore, to unequivocally associate potential differences in fluorescence to individual bacteria, we applied single-cell analyses to apoplast-extracted bacteria. Microscopic analysis on apoplast-extracted bacteria carrying the T3SS gene fusions to *gfp* revealed strong cell-to-cell differences in fluorescence, supporting that expression of the T3SS genes is phenotypically heterogeneous within the plant (Fig. 1C and 1D). Bacteria not expressing the genes were found for all three fusions both by microscopic examination (Fig. 1C), and by flow cytometry analyses (Fig. 1D), indicating that a subpopulation of bacteria that do not express the T3SS genes does appear during colonization of the host plant tissue.

P. syringae bifurcates into two subpopulations due to bistable expression of T3SS genes

To ascertain whether the phenotypic heterogeneity observed for expression of the T3SS genes was a response to environmental cues or could have stochastic origin, we examined gene expression in the homogeneous environment of nutrient-limited Hrp-inducing medium (HIM) (Huynh et al., 1989) (Fig. 2). Growth in HIM triggers a signalling cascade that activates expression of HrpL, which in turn activates expression of all T3SS genes (Fig. 2A and B). A remarkable observation, however, was that all three expression patterns were heterogeneous in HIM, in contrast with those obtained in non-inducing medium (*i.e*. LB medium, Fig. S3). Heterogeneity was higher during exponential growth (24h) than in stationary phase (48h) (Fig. 2B). In all cultures, a fraction of

bacterial cells carrying *gfp* fusions displayed fluorescence levels overlapping with those of non-GFP control bacteria (Fig. 2B, centre and right panels). This was particularly clear in exponentially growing bacteria (24h), where expression of all three *gfp* fusions reached a bistable state (Fig. 2B, centre panels). Because the differences in T3SS expression between the two subpopulations were not all-or-none, we use the terms $TSS3^{HIGH}$ and $T3SS^{LOW}$ instead of $T3SS^{ON}$ and $T3SS^{OFF}$. Bistability was no longer detected in stationary phase cultures (48h), supporting a reversible and non-genetic origin for the differences observed between subpopulations (Fig. 2B, right panels).

Bistability of the T3SS genes requires HrpL and is established through the HrpV/HrpG double-negative regulatory loop

Because HrpL activates expression of *hrcU and hopAB1* (Xiao and Hutcheson, 1994) (Fig. 2A), we considered the possibility that the bistable state might be passed down from HrpL to genes under its control. To test this hypothesis, we introduced into the strains carrying *hrpL::gfp* or *hopAB1::gfp* fusions, a plasmid carrying a copy of *hrpL* under the control of the *lacZ* promoter, which enables moderate, constitutive expression in *P. syringae* (Ortiz-Martín et al., 2010b), to evaluate its impact on *gfp* expression by flow cytometry (Fig. 3A). The bimodal distribution of *hrpL::gfp* expression (Fig. 3A in black) becomes unimodal in the presence of constitutively expressed HrpL (coloured). In the case of *hopAB1::gfp*, bistability is reduced, although not entirely abolished in the presence of plasmid-encoded HrpL, but the population displays a shift towards the $T3SS^{HIGH}$ state. These observations suggest that HrpL may play a central role in the establishment of bistability in the system.

Bistability is often triggered by transforming a quantitative cell-to-cell difference into a qualitative difference through the action of one or more feedback loops (Veening et al., 2008). Two such feedback loops regulate the expression of the T3SS genes in *P. syringae*: (i) a positive feedback loop controlled by HrpA, the main subunit of the T3SS pilus (Roine et al., 1997; Wei et al., 2000); (ii) a double negative feedback loop regulated by HrpV and HrpG (Wei et al., 2005) (Fig. 2A). We analysed the roles of these regulators in the establishment of T3SS bistability using mutants defective in these genes and/or plasmids carrying the individual genes under study. Although bistability in *hopAB1::gfp* expression was reduced in a Δ*hrpA* mutant, bimodal expression of the *hrpL::gfp* fusion was still observed in the absence of HrpA, thus making HrpA an unlikely candidate to be the molecular switch required to trigger the bistable state (Fig. 3B).

Bistability of *hopAB1::gfp* was abolished in a Δ*hrpG* mutant (Fig. 3C). In turn, absence of HrpV increased the proportion of cells expressing higher levels of *hopAB1::gfp* (Fig. 3C). This happened regardless of the presence of HrpG, as indicated by the fact that a Δ*hrpV* mutation was epistatic over a Δ*hrpG* mutation. Constitutive expression of either regulator from a plasmid led to reciprocal results on *hopAB1::gfp* expression: a stronger bistable phenotype was detected upon overexpression of HrpG, and bistability was abolished in cultures that constitutively expressed HrpV (Fig. 3C). The effect that constitutive expression of these regulators have on *hrpL::gfp* closely matched the effect seen on *hopAB1::gfp* (Fig. 4B). A tentative interpretation of the above observations is that HrpG and HrpV may be key elements in T3SS bistability,

perhaps due to the existence of cell-to-cell differences in the amount or activity of these regulators.

Differences in gene expression correlate with differences in virulence

Validation of our reductionist observations in HIM was pursued by analysis *in planta*. In *P. syringae*, the T3SS is necessary to suppress basal defences and T3SS absence limits bacterial proliferation within the plant and prevents the development of disease (Alfano and Collmer, 1997). Thus, if heterogeneous expression of the T3SS genes were associated to the heterogeneity observed in the size of apoplast-located microcolonies, $T3SS^{HIGH}$ and $T3SS^{LOW}$ subpopulations would be expected to differ in their ability to interact with the plant host. To test this possibility, we analysed the development of disease in leaves inoculated with $T3SS^{HIGH}$ and $T3SS^{LOW}$ bacterial subpopulations, sorted according to their level of expression of *hopAB1* (Fig. 4A, upper panel). The sorted populations were both virulent, an observation consistent with the fact that bacteria expressing *hopAB1* were detected in both subpopulations although in different numbers (Fig. 4A, centre panel and 4B). However, the development of disease symptoms was faster in leaf areas inoculated with the population expressing higher levels of *hopAB1,* and the symptoms were also stronger (Fig. 4B). The spread of the disease symptoms was also faster beyond the areas inoculated with the $T3SS^{HIGH}$ subpopulation, suggesting a more efficient colonization of distal tissues by this population. Thus, differences in T3SS gene expression appear to correlate with differences in virulence: namely, the $T3SS^{HIGH}$ subpopulation is more virulent than the $T3SS^{LOW}$ subpopulation.

DISCUSSION

This study shows that colonisation of the plant apoplast by *Pseudomonas syringae* involves cell-to-cell differences in expression of its T3SS. Although microenvironments within the apoplast might provide different signals to control bacterial gene expression, heterogeneous T3SS expression is also detected in the homogeneous environment of nutrient-limited T3SS-inducing medium (HIM), thus making unlikely it results as a direct response to environmental cues. Flow cytometry analysis of cultures grown in HIM showed the occurrence of two bacterial lineages, one of which expressed the T3SS at high levels while the other did not show significant T3SS expression. This bistable pattern of gene expression appeared during exponential growth, and reverted to unimodal heterogeneity in stationary cultures, thus suggesting a non-genetic origin and making phase variation an unlikely one (van der Woude, 2011).

A key factor in bistable expression of the *P. syringae* T3SS appears to be the HrpL sigma factor (Fouts et al., 2002), as indicated by the disappearance of the $T3SS^{LOW}$ subpopulation when expression of HrpL was uncoupled from its regulation (*i.e*. upon constitutive expression of HrpL from a plasmid). HrpL activates expression of more than 50 genes within the nutrient-limited plant leaf apoplast (Ferreira et al., 2006; Lam et al., 2014; Mucyn et al., 2014), including the *hrp/hrc* genes that encode the T3SS, and effector genes (Xiao et al., 1994; Fouts et al., 2002). Bistable expression was detected in *hrcU*, which encodes a structural component of the T3SS required for secretion and translocation (Charkowski et al., 1997), and in *hopAB1*, encoding a type III secreted effector involved in suppression of plant defences (Jackson et al., 1999). Hence,

transmission of HrpL bistability appears to occur downstream the regulatory cascade, generating $T3SS^{HIGH}$ and $T3SS^{LOW}$ cells.

Bistability is hindered either by deletion of *hrpG* or by constitutive expression of HrpV (Fig. 3C), suggesting that the HrpV/HrpG pair may constitute the bistable switch involved in turning quantitative differences in gene expression into qualitative differences. Although HrpA does not seem to be essential, it may contribute to bistability by increasing the number of bacteria with gene expression levels high enough to cross the threshold for activation.

Heterogeneous expression of the *P. syringae* T3SS is also observed during growth within the apoplast, and $T3SS^{HIGH}$ and $T3SS^{LOW}$ cells are recovered from *P. syringae* apoplast colonies. This observation, together with the fact that $T3SS^{HIGH}$ and $T3SS^{LOW}$ subpopulations differ in virulence, suggests that heterogeneous T3SS expression may play a role in the adaptation of *P. syringae* to plant hosts. Unfortunately, a direct test is not feasible because genetic changes that abrogate bistability in laboratory medium (mutation of *hrpG* or plasmid-borne expression of HrpL or HrpV) alter T3SS expression mean levels in a way that impairs virulence (Ortiz-Martín et al., 2010b; Ortiz-Martín et al., 2010a).

While the ultimate significance of T3SS heterogeneity in *P. syringae* remains to be established, a tentative interpretation is that heterogeneous expression of virulence determinants may serve as a stealth strategy for defence evasion in the apoplast, an environment where unsuppressed plant defences are operative (Mitchell et al., 2015). This possibility is supported by theoretical studies indicating that phenotypic heterogeneity can have adaptive value in changing and/or hostile environments (Kussell et al., 2005; Kussell and Leibler, 2005),

298 and by experimental evidence of host defence evasion by lineage formation in
299 animal pathogens (Srikhanta et al., 2010; Lovell et al., 2011; Hernández et al.,
300 2012; Claudi et al., 2014; Sánchez-Romero and Casadesús, 2014; Manina et
301 al., 2015). Moreover, the phenotypic heterogeneity observed in *P. syringae*
302 T3SS genes could also play a role in adaptation to other stages of its life cycle.
303 Among plant pathogens, high frequencies of T3SS polymorphism are detected
304 in natural *Arabidopsis*-associated populations of *P. syringae*, and less
305 aggressive variants, increase their growth potential in mixed infections and have
306 a fitness advantage in non-host environments (Barrett et al., 2011). Furthermore
307 natural isolates of *P. syringae* from agricultural and non-agricultural niches
308 display differences in the phenotypic (but not the genotypic) structure of the
309 populations (Morris et al., 2008). On these grounds, we tentatively propose that
310 phenotypic heterogeneity in T3SS gene expression may protect *P. syringae*
311 populations from plant defences. Furthermore, it seems conceivable that
312 $T3SS^{LOW}$ subpopulations may persist undetected in plant leaves, in a fashion
313 reminiscent of the animal pathogens that cause persistent and chronic
314 infections. Whatever the case, our description of bistable expression of the *P.*
315 *syringae* T3SS brings about the notion that subpopulation formation during
316 infection is not restricted to animal pathogens.
317

EXPERIMENTAL PROCEDURES

Bacterial strains and growth conditions

Bacterial strains used in this work are listed in Table S1, and plasmids are listed in Table S2**.** *Escherichia coli* and *Pseudomonas syringae* pv. *phaseolicola* (*Pph*) were grown at 37°C and 28°C, respectively, with aeration in Lysogeny Broth (LB) medium (Bertani, 1951) or Hrp-inducing medium (HIM) at pH 5.7 (Huynh et al., 1989). Solid media contained agar at a final concentration of 15%. Antibiotics were used at the following concentrations: ampicillin (Amp), 100 μg/ml for *E. coli* DH5α, kanamycin (Km), 50 μg/ml for *E. coli* DH5α and 15 μg/ml for *Pph* 1448A derivative strains.

Fluorescent labelling of bacterial strains

Constitutively expressed fluorescent reporter gene eYFP was introduced into the chromosome of *Pph* strains 1448A using a Tn*7* delivery system (Lambertsen et al., 2004). Bacterial strains carrying chromosome-located transcriptional fusions to a promoterless *gfp* gene of the *hrp* genes *hrpL, hrcU* and *hopAB1* were generated using an adaptation of a previously described method (Zumaquero et al., 2010). The *hrpL* and *hopAB1* genes are encoded as monocistronic units, while *hrcU* is the last gene of an operon (Rahme et al., 1991; Xiao and Hutcheson, 1994; Jackson et al., 2000). For each gene, two fragments of approximately 500 bp were amplified from *Pph* 1448A genomic DNA using iProof High-Fidelity DNA Polymerase (Bio-Rad, USA); one fragment corresponding to the 3' end of the ORF, including the STOP codon, and the other corresponding to the sequence immediately downstream the STOP codon. Primers used are listed in Table S3. The fragments obtained were used

343 in a PCR reaction without additional primers or template, generating single
344 fragments including the end of each ORF and its downstream sequences
345 separated by an *Eco*RI site, which were A/T cloned into pGEM-T (Promega,
346 USA) and fully sequenced to discard mutations, giving raise to pDLM3
347 (p*hopAB1-Eco*RI), pDLM4 (p*hrcU-Eco*RI), and pDLM5 (p*hrpL-Eco*RI).
348 Plasmid pZEP07 (Hautefort et al., 2008) was used to amplify a fragment
349 containing a promoterless *gfp* gene carrying its own ribosomal-binding site
350 (Willmann et al., 2011), followed by an *Eco*RV site and chloramphenicol
351 resistance cassette. This fragment was A/T cloned into pGEM-T (Promega,
352 USA) generating pDLM1. The *nptII* kanamycin resistance gene, flanked by FRT
353 sites (Flippase Recognition Target), was PCR-amplified using pDOC-K (Lee et
354 al., 2009) as a template, and cloned into the *Eco*RV site from pDLM1, to
355 generate pDLM2. pDLM2 was used to amplify a fragment containing the
356 promoterless *gfp* gene with its RBS, the kanamycin resistance gene, and the
357 chloramphenicol resistance gene, and the fragment obtained cloned into
358 pDLM3, pDLM4 and pDLM5, digested with *Eco*RI and treated with the Klenow
359 polymerase fragment (Takara, Japan) generating plasmids pDLM6, pDLM7 and
360 pDLM8, respectively. These resulting plasmids were introduced into *Pph* 1448A
361 and derivatives, as previously described (Zumaquero et al., 2010). Southern
362 blot analysis, using the *nptII* gene as a probe, was used to confirm that allelic
363 exchange occurred at a single and correct position within the genome.
364
365 **Plant growth and inoculation**
366 *Phaseolus vulgaris* bean cultivar Canadian Wonder plants were grown at 23°C,
367 95% humidity, with artificial light maintained for 16-h periods within the 24-h

cycle. For inoculum preparation, bacterial lawns were grown on LB plates for 48 h at 28°C and resuspended in 2 mL of 10 mM $MgCl_2$. The OD_{600} was adjusted to 0.1 (5 x 10^7 colony forming units or cfu/mL) and serial dilutions made to reach the final inoculum concentration.

Infiltration of bean leaves for confocal microscopy or symptom development was carried out using a needless syringe and a 5 x 10^6 cfu/ml bacterial suspension in 10 mM $MgCl_2$. Infiltration of bean leaves to be analysed for flow cytometry was carried out after dipping a whole leaf into a 5 x 10^8 cfu/ml bacterial solution in 0.01% Silwett L-77 (Crompton Europe Ltd, Evesham, UK), using a pressure chamber. Five days post inoculation (dpi) bacteria were recovered from the plant by an apoplastic fluid extraction. The apoplastic fluid extraction was carried out by pressure infiltrating a whole leaf with 10 ml of a 10 mM $MgCl_2$ solution inside a 20 ml syringe. Following 5 cycles of pressure application, the flow-through was removed and placed in a fresh 50 ml tube, and the leaf retained within the syringe was introduced into another 50 ml tube. Both tubes were centrifuged for 30 min at low speed (900 *g*) at 4ºC. Pellets were resuspended into 1 ml of $MgCl_2$ and analysed by flow cytometry.

Flow Cytometry and Cell Sorting

Five hundred µl of an overnight *P. syringae* LB culture was washed twice in 10 mM $MgCl_2$ and added to 4.5 ml of HIM. Cultures and apoplast-extracted bacterial suspensions were analysed using a BD FACSVerse cytometer and the BD FACSuite software (BD Biosciences) after incubation at 28ºC. Stationary cultures were sorted using a MoFloTM XDP cytometer (Beckman Coulter). Immediately before sorting, 5 x 10^6 cells were analysed for GFP fluorescence.

Based on this analysis, gates were drawn to separate the cells displaying fluorescence levels overlapping the 1448A non-GFP bacterial population used as a negative control, from cells expressing higher GFP levels, as indicated in the corresponding histogram. From each gate, cells were collected into a sterile tube. After sorting, cells were spun at 12,000 *g* for 10 min, and the resulting pellets resuspended into 10mM $MgCl_2$, and bacterial concentration adjusted to 1 x 10^6 cfu/ml. An aliquot of sorted cells was run again at the cytometer to confirm the differences in expression of the separated populations. Data were analysed with FlowJo Software. All experiments included two replicate samples and a number of independent experiments carried out as indicated for each figure, which shows typical results.

Microscopy

Sections of inoculated *P. vulgaris* leaves (approximately 5 mm^2) were excised with a razor blade, and mounted on slides in double-distilled H_2O (lower epidermis toward objective) under a 0.17 mm coverslip. Images of the leaf mesophyll and apoplast-extracted bacteria were taken using the Leica SP5 II confocal microscope (Leica Microsystems GmbH, Wetzlar, Germany). Apoplast-extracted bacteria were stained with FM4-64 at 20 µM (Life Technologies).

Variable AOTF filters were used for the visualization of the following fluorophores (excitation/ emission): eYFP (514 nm/ 525 to 600 nm), GFP (488 nm/ 500 to 533 nm), FM4-64 (488 nm/ 604-674 nm) plant autofluorescence (514/ 605 to 670 nm). Z series imaging were taken at 1 µm or 10 µm intervals when using 40x or 10x objectives respectively. Image processing was performed using Leica LAS AF (Leica Microsystems). Colony area was

418 calculated using Fiji distribution of ImageJ software. All experiments included
419 two replicate samples and a number of independent experiments carried out as
420 indicated for each figure, which shows typical results.
421

ACKNOWLEDGMENTS

We are grateful to David Navas (Servicios Centrales de Apoyo a la Investigación, Universidad de Málaga), Alberto Álvarez and Pilar Torralbo (Servicio de Técnicas Aplicadas a la Biociencia, Universidad de Extremadura, Badajoz), Modesto Carballo, Laura Navarro, and Cristina Reyes (Servicio de Biología, Centro de Investigación Tecnológica e Innovación, Universidad de Sevilla, Sevilla), and to Pablo Vallejo for technical assistance. We wish to thank E.R. Bejarano and A. Castillo for their helpful comments and suggestions. We also wish to thank David W. Holden for his critical reading of the manuscript. This work was supported by grants from the Ministerio de Ciencia e Innovación (MICINN, Spain; BIO2009-11516) and Ministerio de Economía y Competitividad (MINECO, Spain) BIO2012-35641 to C.R. Beuzón, and BIO2015-64391-R to C.R. Beuzón and J. Ruiz-Albert. J.S. Rufián has been supported by a FPI fellowship associated with a grant of E.R. Bejarano (MICINN, Spain; AGL2010-22287-C02-2), funds from BIO2012-35641, and Plan Propio de la Universidad de Málaga – Andalucía Tech. The work was co-funded by European Regional Development Funds (FEDER).

FIGURE LEGENDS

Figure 1. Colony development and T3SS gene expression in *P. syringae* display phenotypic heterogeneity within the plant. (**A and B**) Colony development is phenotypically heterogeneous within the plant apoplast. (**A**) Representative confocal microscopy image of bean leaves inoculated with $5x10^6$ cfu/ml of wild type eYFP (yellow) 3 days post-inoculation (dpi). Boxes highlight small microcolonies among the typical and more abundant larger ones. Largest not-rounded microcolonies typically result from closely located colonies merging. Red corresponds to auto-fluorescence generated by chloroplasts. Scale bar corresponds to 100 µm. At least three independent experiments were carried out (**B**). Graph showing relative area of individual microcolonies. Colony area is expressed in percentage of total image area. (**C and D**) Expression of the T3SS is phenotypically heterogeneous within the plant. (**C**) Fluorescence microscopy images of apoplast-extracted bacteria from bean leaves 5 days post-inoculation with a $5x10^5$ cfu/ml inoculum of each of the strains carrying chromosome-located transcriptional *gfp* fusions to the T3SS genes *hrpL, hrcU* or *hopAB1*. Left panels show GFP fluorescence, and right panels this image merged with that obtained from bacterial staining with the membrane dye FM4-64 (red). Inset shows a close up of the area of the corresponding image enclosed by a solid line square. Dotted line squares highlight other examples of bacteria displaying GFP fluorescence below the level of detection. Scale bar corresponds to 10 µm. (**D**) Flow cytometry analysis of apoplast-extracted bacteria carrying *hrpL::gfp, hrcU::gfp* or *hopAB1::gfp* fusions, obtained from bean leaves 5 days after inoculation with a $5x10^5$ cfu/ml inoculum. Non-GFP 1448A was also included as a reference to differenciate OFF and ON

subpopulations. Data are represented as a dot plot (forward scatter [cellular size] *versus* GFP fluorescence intensity). All data were collected for 100,000 events per sample. At least three independent experiments with two replicates each were carried out. Figure shows typical results.

Figure 2. Expression of *hrpL::gfp*, *hrcU::gfp* and *hopAB1::gfp* is bistable during exponential growth in Hrp-inducing medium. (**A**) Schematic representation of the two feedback regulatory loops operating on the expression of the T3SS genes: a positive feedback loop controlled by HrpA, and a double negative feedback loop regulated by HrpV, an anti-activator of the T3SS genes that binds to HrpS the enhancer-binding protein required for HrpL expression, and HrpG, which binds to HrpV acting as an anti-anti-activator. Expression of *hrpA*, *hrpV*, *hrpG*, *hrcU*, and *hopAB1*, is HrpL-activated, although in the case of highly expressed *hopAB1* some expression can still be detected in the absence of HrpL. (**B**) Histograms show flow cytometry analysis of strains carrying chromosome-located transcriptional fusions to the T3SS genes *hrpL* (top row), *hrcU* (middle row) or *hopAB1* (bottom row). Histograms show cell counts *versus* GFP fluorescence at 0h (immediately after a 1:10 dilution into HIM of an overnight LB culture), 24h after the dilution into HIM (exponential phase) or 48h (stationary phase). Black histograms show non-GFP 1448A included as a reference. Coloured histograms show GFP fluorescence for the strains carrying the fusions as indicated in each case. Dotted lines show the results of a replicate experiment. All data were collected for 100,000 events per sample. At least three independent experiments with two replicates each were carried out. Figure shows typical results.

Figure 3. Bistability of *hrpL::gfp* and *hopAB1::gfp* is abolished by constitutive expression of HrpL, deletion of *hrpG* or constitutive expression of HrpV. (**A**) Flow cytometry analysis of HIM-growing bacterial strains carrying chromosome-located transcriptional fusions to the T3SS genes *hrpL* or *hopAB1*, carrying or not a plasmid expressing *hrpL* under the control of P_{lac}, a constitutive promoter of moderate expression in *P. syringae*. Histograms show cell counts *versus* GFP fluorescence after 24h of growth in HIM. Black histograms show fluorescence of the fusions in the absence of the plasmid. Coloured histograms show fluorescence of the fusions in the strain carrying the plasmid as indicated. Dotted lines show the results of a replicate experiment. (**B**) Flow cytometry analysis of HIM-growing bacterial strains carrying chromosome-located transcriptional fusions to the T3SS genes *hrpL* or *hopAB1*, in different genetic backgrounds. Histograms show cell counts *versus* GFP fluorescence after 24h of growth in HIM. Black histograms show fluorescence of the fusions in an otherwise wild type background. Coloured histograms show fluorescence of the fusions in a strain carrying the Δ*hrpA* mutation. Dotted lines show the results of a replicate experiment. All data were collected for 100,000 events per sample. (**C**) Flow cytometry analysis of HIM-growing bacterial strains carrying chromosome-located transcriptional fusions to the T3SS genes *hopAB1 or hrpL*, in different genetic backgrounds. Histograms show cell counts *versus* GFP fluorescence after 24h of growth in HIM. Histograms show fluorescence of the fusions in each of the indicated genetic backgrounds. WT indicate the strain that only carries the indicated gene fusion. All data were collected for 100,000 events per sample. At least two independent experiments with two replicates each were carried out with similar results.

Figure 4. Bacterial populations sorted according to *hopAB1* expression display differences in virulence. (**A**) Flow cytometry analysis of a HIM-growing culture of the strain carrying *hopAB1::gfp*. GFP fluorescence intensity is shown as a green histogram. Gates were drawn to separate *hopAB1::gfp* bacteria displaying fluorescence levels overlapping the 1448A non-GFP bacterial population (indicated with a line marked as low), used as a negative control (Grey histogram), from cells expressing high GFP levels (indicated with a line marked as high, and including the mode for the expressing population). After sorting, aliquots of sorted cells were run again through the cytometer to confirm the efficacy of the sorting process (below), and bacterial concentration adjusted to 1 x 10^6 cfu/ml. Some overlap caused by the dynamic and reversible nature of the process can be detected (**B**) Disease symptom progression in bean leaves inoculated with 1 x 10^6 cfu/ml of each of the sorted populations at 6 and 11 days post inoculation (dpi). Results from three replicate experiments are shown.

Supplemental figures

Figure S1. Strains carrying transcriptional fusions to gfp of hrpL, hrcU or hopAB1 display wild type virulence. Symptom development 7 days post inoculation of a bean leaf with 5x10^5 cfu/ml or either wild type Pph 1448A or each of its derivatives carrying the indicated gene fusions.

Figure S2. **Bacterial colonies display heterogeneous distribution of *gfp* fluorescence that cannot be unequivocally associated to individual cells.** Confocal microscopy images showing bacterial microcolonies within the apoplast of bean leaves, 5 days post-inoculation with 5x10^6 cfu/ml of each of the strains carrying the chromosome-located transcriptional *hrpL::gfp, hrcU::gfp*

or *hopAB1::gfp* fusions. Red corresponds to auto-fluorescence generated by chloroplasts. Scale bar corresponds to 50 µm.

Figure S3. Flow cytometry analysis of in LB-grown bacterial cultures. Histograms of GFP fluorescence distribution in the strains carrying the chromosome-located transcriptional *hrpL::gfp, hrcU::gfp* or *hopAB1::gfp* fusions growing at 24h (**A**) or 48h (**B**). Grey histograms show a strain not expressing GFP. All data was collected for 100,000 events per sample.

Video S1 and S2 3D reconstructions of 1 µm z-stack confocal images showing the uneven distribution of bacteria within two different apoplast-located microcolonies of Pph 1448A constitutively expressing GFP. Bean leaves were inoculated with $5x10^5$ cfu/ml, and visualized 3 days post inoculation.

References

Alfano, J.R., and Collmer, A. (1997) The type III (Hrp) secretion pathway of plant pathogenic bacteria: trafficking harpins, Avr proteins, and death. *J Bacteriol* **179**: 5655-5662.

Arnoldini, M., Vizcarra, I.A., Pena-Miller, R., Stocker, N., Diard, M., Vogel, V. et al. (2014) Bistable expression of virulence genes in salmonella leads to the formation of an antibiotic-tolerant subpopulation. *PLoS Biol* **12**: e1001928.

Barrett, L.G., Bell, T., Dwyer, G., and Bergelson, J. (2011) Cheating, trade-offs and the evolution of aggressiveness in a natural pathogen population. *Ecol Lett* **14**: 1149-1157.

Bäumler, A.J., Winter, S.E., Thiennimitr, P., and Casadesús, J. (2011) Intestinal and chronic infections: *Salmonella* lifestyles in hostile environments. *Environ Microbiol Rep* **3**: 508-517.

Bertani, G. (1951) Studies on lysogenesis. I. The mode of phage liberation by lysogenic Escherichia coli. *J Bacteriol* **62**: 293-300.

Bigger, J. (1944) Treatment of Staphylococcal infections with penicillin by intermittent sterilisation. *Lancet* **244**: 497-500.

Bram Van den Bergh, J.E.M., Tom Wenseleers, Etthel M. Windels, Pieterjan Vanden Boer, Donaat Kestemont, Luc De Meester, Kevin J. Verstrepen, Natalie Verstraeten, Maarten Fauvart & Jan Michiels (2016) Frequency of antibiotic application drives rapid evolutionary adaptation of Escherichia coli persistence. *Nature Microbiology* **1**.

Brian P. Conlon, S.E.R., Autumn Brown Gandt, Austin S. Nuxoll, Niles P. Donegan, Eliza A. Zalis, Geremy Clair, Joshua N. Adkins, Ambrose L. Cheung & Kim Lewis (2016) Persister formation in Staphylococcus aureus is associated with ATP depletion. *Nature Microbiology* **1**.

Campbell-Valois, F.X., Schnupf, P., Nigro, G., Sachse, M., Sansonetti, P.J., and Parsot, C. (2014) A fluorescent reporter reveals on/off regulation of the Shigella type III secretion apparatus during entry and cell-to-cell spread. *Cell Host Microbe* **15**: 177-189.

Charkowski, A.O., Huang, H.C., and Collmer, A. (1997) Altered localization of HrpZ in *Pseudomonas syringae* pv. *syringae* hrp mutants suggests that different components of the type III secretion pathway control protein translocation across the inner and outer membranes of gram-negative bacteria. *J Bacteriol* **179**: 3866-3874.

Claudi, B., Sprote, P., Chirkova, A., Personnic, N., Zankl, J., Schurmann, N. et al. (2014) Phenotypic variation of *Salmonella* in host tissues delays eradication by antimicrobial chemotherapy. *Cell* **158**: 722-733.

Davidson, C.J., and Surette, M.G. (2008) Individuality in bacteria. *Annu Rev Genet* **42**: 253-268.

Davis, K.M., Mohammadi, S., and Isberg, R.R. (2015) Community behavior and spatial regulation within a bacterial microcolony in deep tissue sites serves to protect against host attack. *Cell Host Microbe* **17**: 21-31.

Dubnau, D., and Losick, R. (2006) Bistability in bacteria. *Mol Microbiol* **61**: 564-572.

Ferreira, A.O., Myers, C.R., Gordon, J.S., Martin, G.B., Vencato, M., Collmer, A. et al. (2006) Whole-genome expression profiling defines the HrpL regulon of *Pseudomonas syringae* pv. *tomato* DC3000, allows de novo reconstruction of

599 the Hrp *cis* element, and identifies novel coregulated genes. *Mol Plant Microbe*
600 *Interact* **19**: 1167-1179.
601 Fouts, D.E., Abramovitch, R.B., Alfano, J.R., Baldo, A.M., Buell, C.R.,
602 Cartinhour, S. et al. (2002) Genomewide identification of *Pseudomonas*
603 *syringae* pv. tomato DC3000 promoters controlled by the HrpL alternative sigma
604 factor. *Proc Natl Acad Sci* **99**: 2275-2280.
605 Green, S., Studholme, D.J., Laue, B.E., Dorati, F., Lovell, H., Arnold, D. et al.
606 (2010) Comparative genome analysis provides insights into the evolution and
607 adaptation of *Pseudomonas syringae* pv. *aesculi* on *Aesculus hippocastanum*.
608 *PLoS One* **5**: e10224.
609 Hautefort, I., Thompson, A., Eriksson-Ygberg, S., Parker, M.L., Lucchini, S.,
610 Danino, V. et al. (2008) During infection of epithelial cells *Salmonella enterica*
611 serovar Typhimurium undergoes a time-dependent transcriptional adaptation
612 that results in simultaneous expression of three type 3 secretion systems. *Cell*
613 *Microbiol* **10**: 958-984.
614 Helaine, S., and Holden, D.W. (2013) Heterogeneity of intracellular replication
615 of bacterial pathogens. *Curr Opin Microbiol* **16**: 184-191.
616 Hernández, S.B., Cota, I., Ducret, A., Aussel, L., and Casadesús, J. (2012)
617 Adaptation and preadaptation of *Salmonella enterica* to Bile. *PLoS Genet* **8**:
618 e1002459.
619 Herskowitz, I., and Hagen, D. (1980) The lysis-lysogeny decision of phage
620 lambda: explicit programming and responsiveness. *Annu Rev Genet* **14**: 399-
621 445.
622 Huynh, T.V., Dahlbeck, D., and Staskawicz, B.J. (1989) Bacterial blight of
623 soybean: regulation of a pathogen gene determining host cultivar specificity.
624 *Science* **245**: 1374-1377.
625 Jackson, R.W., Mansfield, J.W., Arnold, D.L., Sesma, A., Paynter, C.D., Murillo,
626 J. et al. (2000) Excision from tRNA genes of a large chromosomal region,
627 carrying *avrPphB*, associated with race change in the bean pathogen,
628 *Pseudomonas syringae* pv. *phaseolicola*. *Mol Microbiol* **38**: 186-197.
629 Jackson, R.W., Athanassopoulos, E., Tsiamis, G., Mansfield, J.W., Sesma, A.,
630 Arnold, D.L. et al. (1999) Identification of a pathogenicity island, which contains
631 genes for virulence and avirulence, on a large native plasmid in the bean
632 pathogen *Pseudomonas syringae* pathovar *phaseolicola*. *Proc Natl Acad Sci*
633 **96**: 10875-10880.
634 Kussell, E., and Leibler, S. (2005) Phenotypic diversity, population growth, and
635 information in fluctuating environments. *Science* **309**: 2075-2078.
636 Kussell, E., Kishony, R., Balaban, N.Q., and Leibler, S. (2005) Bacterial
637 persistence: a model of survival in changing environments. *Genetics* **169**: 1807-
638 1814.
639 Lam, H.N., Chakravarthy, S., Wei, H.L., BuiNguyen, H., Stodghill, P.V., Collmer,
640 A. et al. (2014) Global analysis of the HrpL regulon in the plant pathogen
641 *Pseudomonas syringae* pv. *tomato* DC3000 reveals new regulon members with
642 diverse functions. *PLoS One* **9**: e106115.
643 Lambertsen, L., Sternberg, C., and Molin, S. (2004) Mini-Tn*7* transposons for
644 site-specific tagging of bacteria with fluorescent proteins. *Environ Microbiol* **6**:
645 726-732.
646 Lee, D.J., Bingle, L.E., Heurlier, K., Pallen, M.J., Penn, C.W., Busby, S.J., and
647 Hobman, J.L. (2009) Gene doctoring: a method for recombineering in laboratory
648 and pathogenic *Escherichia coli* strains. *BMC Microbiol* **9**: 252.

649 Lovell, H.C., Jackson, R.W., Mansfield, J.W., Godfrey, S.A., Hancock, J.T.,
650 Desikan, R., and Arnold, D.L. (2011) *In planta* conditions induce genomic
651 changes in *Pseudomonas syringae* pv. *phaseolicola*. *Mol Plant Pathol* **12**: 167-
652 176.
653 Macho, A.P., and Zipfel, C. (2015) Targeting of plant pattern recognition
654 receptor-triggered immunity by bacterial type-III secretion system effectors. *Curr*
655 *Opin Microbiol* **23**: 14-22.
656 Manina, G., Dhar, N., and McKinney, J.D. (2015) Stress and host immunity
657 amplify *Mycobacterium tuberculosis* phenotypic heterogeneity and induce
658 nongrowing metabolically active forms. *Cell Host Microbe* **17**: 32-46.
659 Mansfield, J., Genin, S., Magori, S., Citovsky, V., Sriariyanum, M., Ronald, P. et
660 al. (2012) Top 10 plant pathogenic bacteria in molecular plant pathology. *Mol*
661 *Plant Pathol* **13**: 614-629.
662 Mitchell, K., Brown, I., Knox, P., and Mansfield, J. (2015) The role of cell wall-
663 based defences in the early restriction of non-pathogenic *hrp* mutant bacteria in
664 Arabidopsis. *Phytochemistry* **112**: 139-150.
665 Morris, C.E., Sands, D.C., Vinatzer, B.A., Glaux, C., Guilbaud, C., Buffiere, A. et
666 al. (2008) The life history of the plant pathogen *Pseudomonas syringae* is linked
667 to the water cycle. *ISME J* **2**: 321-334.
668 Mucyn, T.S., Yourstone, S., Lind, A.L., Biswas, S., Nishimura, M.T., Baltrus,
669 D.A. et al. (2014) Variable suites of non-effector genes are co-regulated in the
670 type III secretion virulence regulon across the *Pseudomonas syringae*
671 phylogeny. *PLoS Pathog* **10**: e1003807.
672 Nielsen, A.T., Dolganov, N.A., Rasmussen, T., Otto, G., Miller, M.C., Felt, S.A.
673 et al. (2010) A bistable switch and anatomical site control *Vibrio cholerae*
674 virulence gene expression in the intestine. *PLoS Pathog* **6**: e1001102.
675 Novick, A., and Weiner, M. (1957) Enzyme Induction as an All-or-None
676 Phenomenon. *Proc Natl Acad Sci U S A* **43**: 553-566.
677 Ortiz-Martín, I., Thwaites, R., Mansfield, J.W., and Beuzón, C.R. (2010a)
678 Negative regulation of the Hrp type III secretion system in *Pseudomonas*
679 *syringae* pv. *phaseolicola*. *Mol Plant Microbe Interact* **23**: 682-701.
680 Ortiz-Martín, I., Thwaites, R., Macho, A.P., Mansfield, J.W., and Beuzón, C.R.
681 (2010b) Positive regulation of the Hrp type III secretion system in *Pseudomonas*
682 *syringae* pv. *phaseolicola*. *Mol Plant Microbe Interact* **23**: 665-681.
683 Rahme, L.G., Mindrinos, M.N., and Panopoulos, N.J. (1991) Genetic and
684 transcriptional organization of the hrp cluster of *Pseudomonas syringae* pv.
685 *phaseolicola*. *J Bacteriol* **173**: 575-586.
686 Rohmer, L., Guttman, D.S., and Dangl, J.L. (2004) Diverse evolutionary
687 mechanisms shape the type III effector virulence factor repertoire in the plant
688 pathogen *Pseudomonas syringae*. *Genetics* **167**: 1341-1360.
689 Roine, E., Wei, W., Yuan, J., Nurmiaho-Lassila, E.L., Kalkkinen, N.,
690 Romantschuk, M., and He, S.Y. (1997) Hrp pilus: an *hrp*-dependent bacterial
691 surface appendage produced by *Pseudomonas syringae* pv. *tomato* DC3000.
692 *Proc Natl Acad Sci* **94**: 3459-3464.
693 Saini, S., Koirala, S., Floess, E., Mears, P.J., Chemla, Y.R., Golding, I. et al.
694 (2010) FliZ induces a kinetic switch in flagellar gene expression. *J Bacteriol*
695 **192**: 6477-6481.
696 Sánchez-Romero, M.A., and Casadesús, J. (2014) Contribution of phenotypic
697 heterogeneity to adaptive antibiotic resistance. *Proc Natl Acad Sci U S A* **111**:
698 355-360.

699 Shenge, K.C., Mabagala, R.B., Mortensen, C.N., Stephan, D. and Wydra, K
700 (2007) First report of bacterial speck of tomato caused by *Pseudomonas*
701 *syringae* pv. *tomato* in Tanzania. *Plant Disease* **91**: 462.
702 Srikhanta, Y.N., Fox, K.L., and Jennings, M.P. (2010) The phasevarion: phase
703 variation of type III DNA methyltransferases controls coordinated switching in
704 multiple genes. *Nat Rev Microbiol* **8**: 196-206.
705 Stecher, B., Hapfelmeier, S., Muller, C., Kremer, M., Stallmach, T., and Hardt,
706 W.D. (2004) Flagella and chemotaxis are required for efficient induction of
707 *Salmonella enterica* serovar Typhimurium colitis in streptomycin-pretreated
708 mice. *Infect Immun* **72**: 4138-4150.
709 Stewart, M.K., and Cookson, B.T. (2012) Non-genetic diversity shapes
710 infectious capacity and host resistance. *Trends Microbiol* **20**: 461-466.
711 Uphoff, S., Lord, N.D., Okumus, B., Potvin-Trottier, L., Sherratt, D.J., and
712 Paulsson, J. (2016) Stochastic activation of a DNA damage response causes
713 cell-to-cell mutation rate variation. *Science* **351**: 1094-1097.
714 van der Woude, M.W. (2011) Phase variation: how to create and coordinate
715 population diversity. *Curr Opin Microbiol* **14**: 205-211.
716 van Vliet, S., and Ackermann, M. (2015) Bacterial Ventures into Multicellularity:
717 Collectivism through Individuality. *PLoS Biol* **13**: e1002162.
718 Veening, J.W., Smits, W.K., and Kuipers, O.P. (2008) Bistability, epigenetics,
719 and bet-hedging in bacteria. *Annu Rev Microbiol* **62**: 193-210.
720 Victor I. Band, E.K.C., Brooke A. Napier, Carmen M. Herrera, Greg K. Tharp,
721 Kranthi Vavikolanu, Jan Pohl, Timothy D. Read, Steven E. Bosinger, M.
722 Stephen Trent, Eileen M. Burd & David S. Weiss (2016) Antibiotic failure
723 mediated by a resistant subpopulation in Enterobacter cloacae. *Nature*
724 *Microbiology* **1**.
725 Wei, C.F., Deng, W.L., and Huang, H.C. (2005) A chaperone-like HrpG protein
726 acts as a suppressor of HrpV in regulation of the *Pseudomonas syringae* pv.
727 *syringae* type III secretion system. *Mol Microbiol* **57**: 520-536.
728 Wei, W., Plovanich-Jones, A., Deng, W.L., Jin, Q.L., Collmer, A., Huang, H.C.,
729 and He, S.Y. (2000) The gene coding for the Hrp pilus structural protein is
730 required for type III secretion of Hrp and Avr proteins in *Pseudomonas syringae*
731 pv. *tomato*. *Proc Natl Acad Sci* **97**: 2247-2252.
732 Willmann, R., Lajunen, H.M., Erbs, G., Newman, M.-A., Kolb, D., Tsuda, K. et
733 al. (2011) Arabidopsis lysin-motif proteins LYM1 LYM3 CERK1 mediate
734 bacterial peptidoglycan sensing and immunity to bacterial infection.
735 *Proceedings of the National Academy of Sciences* **108**: 19824-19829.
736 Xiao, Y., and Hutcheson, S.W. (1994) A single promoter sequence recognized
737 by a newly identified alternate sigma factor directs expression of pathogenicity
738 and host range determinants in *Pseudomonas syringae*. *J Bacteriol* **176**: 3089-
739 3091.
740 Xiao, Y., Heu, S., Yi, J., Lu, Y., and Hutcheson, S.W. (1994) Identification of a
741 putative alternate sigma factor and characterization of a multicomponent
742 regulatory cascade controlling the expression of *Pseudomonas syringae* pv.
743 syringae Pss61 *hrp* and *hrmA* genes. *J Bacteriol* **176**: 1025-1036.
744 Zeng, Q., Laiosa, M.D., Steeber, D.A., Biddle, E.M., Peng, Q., and Yang, C.H.
745 (2012) Cell individuality: the bistable gene expression of the type III secretion
746 system in *Dickeya dadantii* 3937. *Mol Plant Microbe Interact* **25**: 37-47.

747 Zumaquero, A., Macho, A.P., Rufián, J.S., and Beuzón, C.R. (2010) Analysis of
748 the role of the type III effector inventory of *Pseudomonas syringae* pv.
749 *phaseolicola* 1448a in interaction with the plant. *J Bacteriol* **192**: 4474-4488.
750

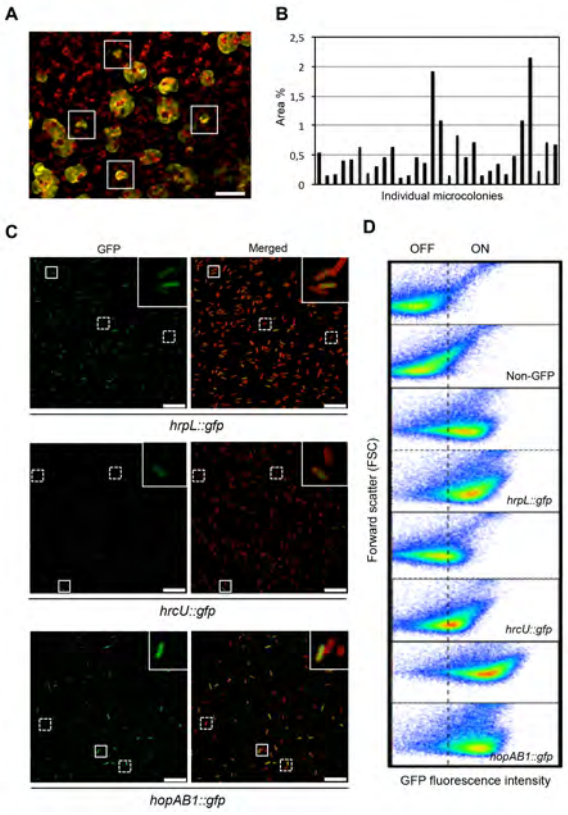
A
B
2,5
2
1,5
1
0,5
0
Area %
Individual microcolonies
C
GFP
Merged
hrpL::gfp
hrcU::gfp
hopAB1::gfp
D
OFF
ON
Non-GFP
hrpL::gfp
hrcU::gfp
hopAB1::gfp
Forward scatter (FSC)
GFP fluorescence intensity

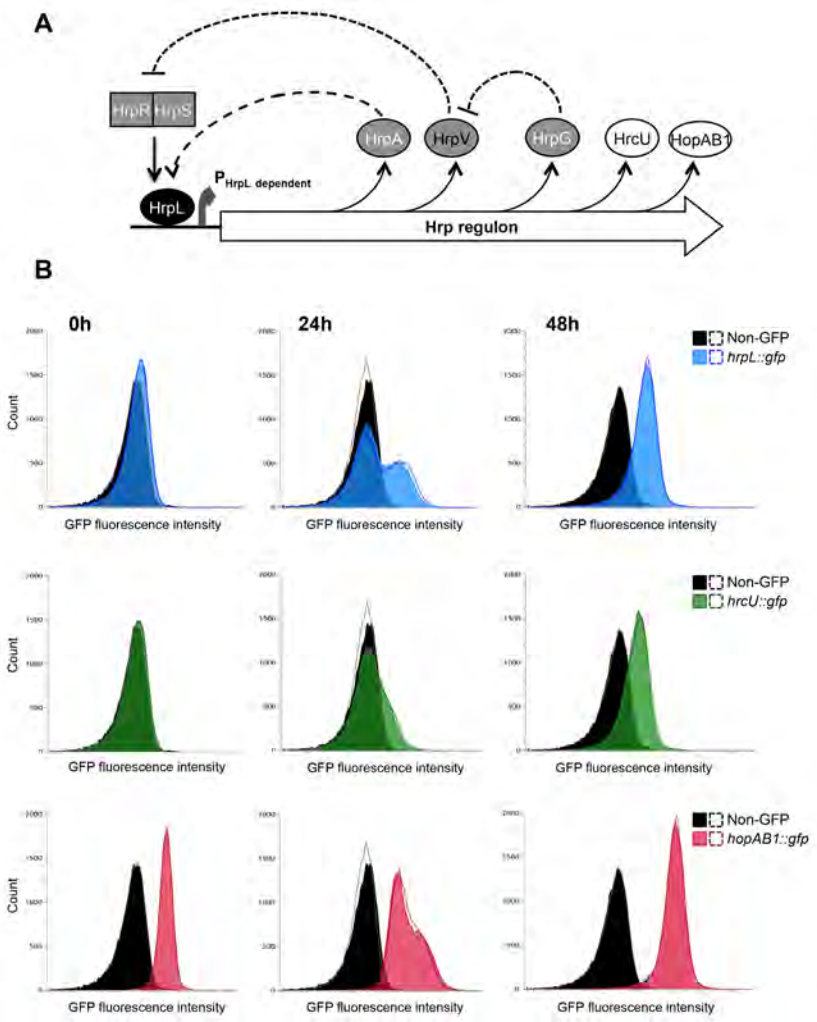
A
HrpR
HrpS
HrpA
HrpV
HrpC
HrcU
HopAB1
P HrpL dependent
HrpL
Hrp regulon
B
0h
24h
48h
Non-GFP
hrpL::gfp
Count
GFP fluorescence intensity
Non-GFP
hrcU::gfp
GFP fluorescence intensity
Non-GFP
hopAB1::gfp
GFP fluorescence intensity

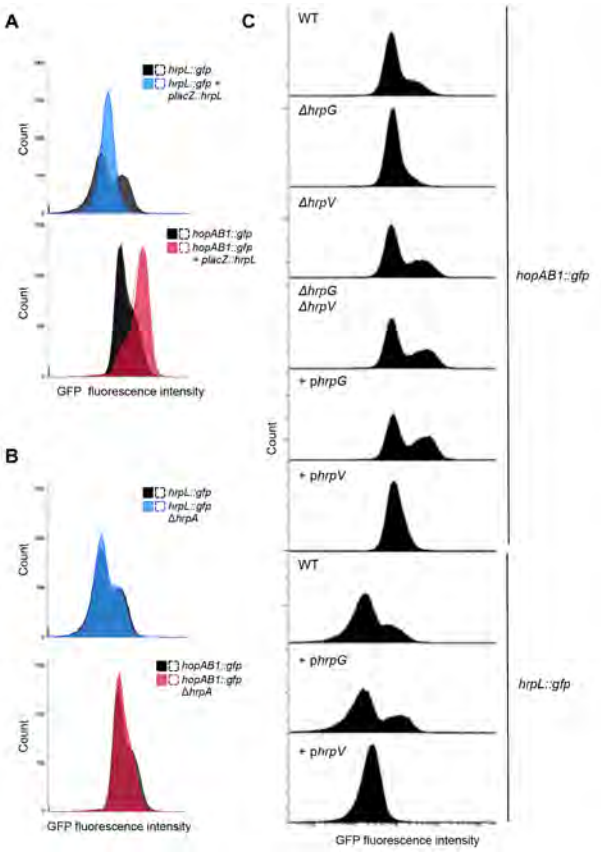
A
hrpL::gfp
hrpL::gfp + placZ::hrpL
Count
hopAB1::gfp
hopAB1::gfp + placZ::hrpL
Count
GFP fluorescence intensity
B
hrpL::gfp
hrpL::gfp ΔhrpA
Count
hopAB1::gfp
hopAB1::gfp ΔhrpA
Count
GFP fluorescence intensity
C
WT
ΔhrpG
ΔhrpV
ΔhrpG ΔhrpV
+ phrpG
+ phrpV
hopAB1::gfp
WT
+ phrpG
+ phrpV
hrpL::gfp
Count
GFP fluorescence intensity

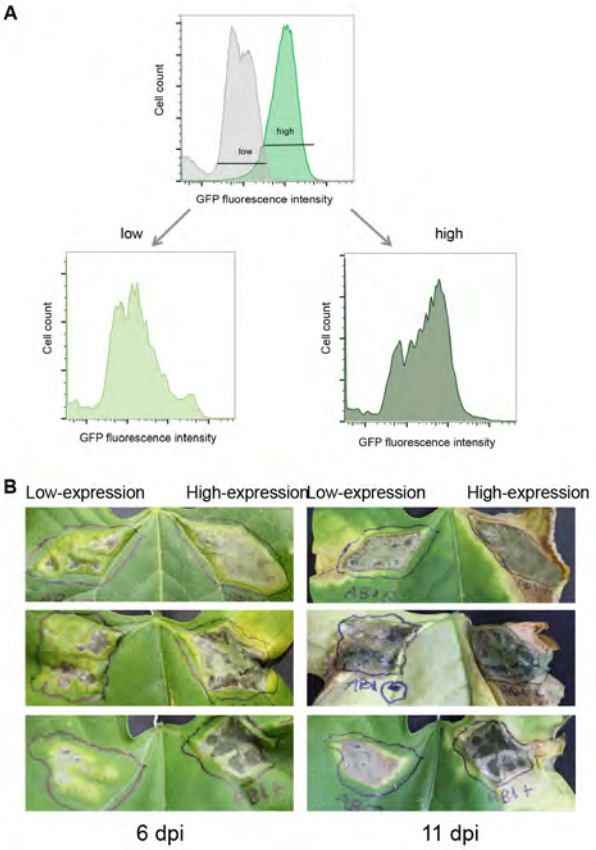
A
Cell count
low
high
GFP fluorescence intensity
low
high
Cell count
GFP fluorescence intensity
Cell count
GFP fluorescence intensity
B
Low-expression
High-expression
Low-expression
High-expression
6 dpi
11 dpi

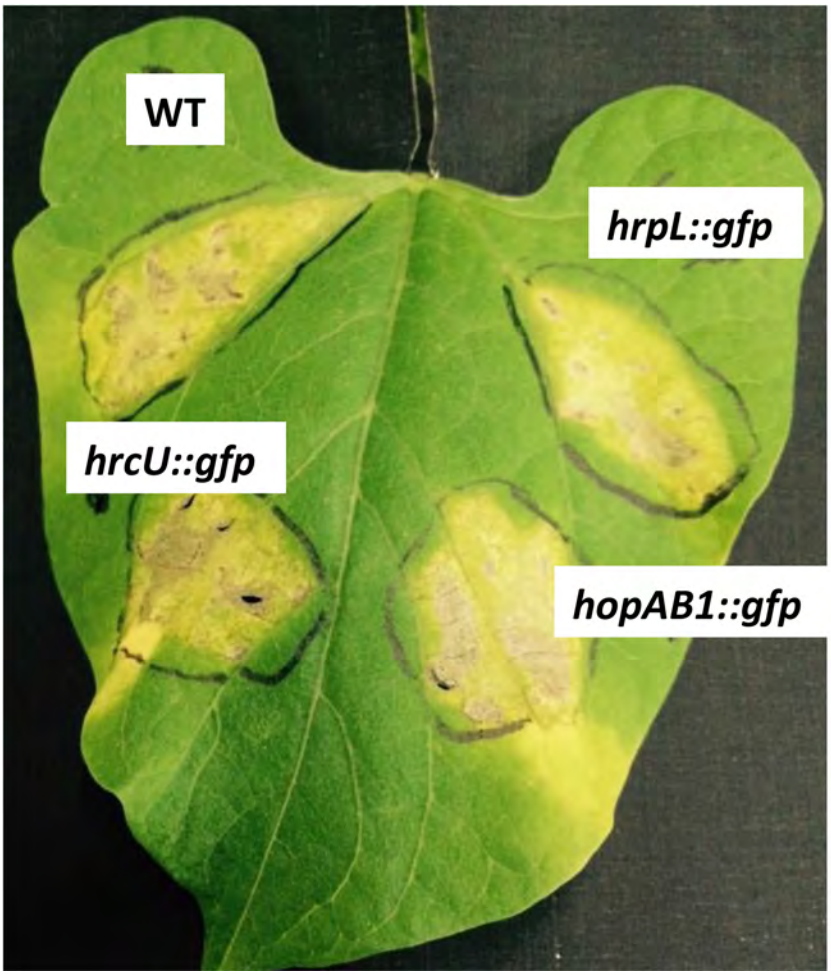
WT
hrpL::gfp
hrcU::gfp
hopAB1::gfp

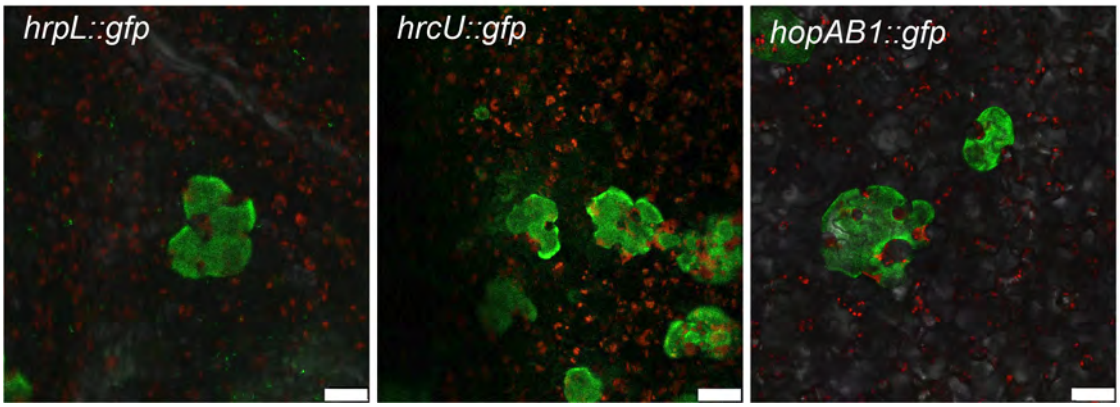
hrpL::gfp
hrcU::gfp
hopAB1::gfp

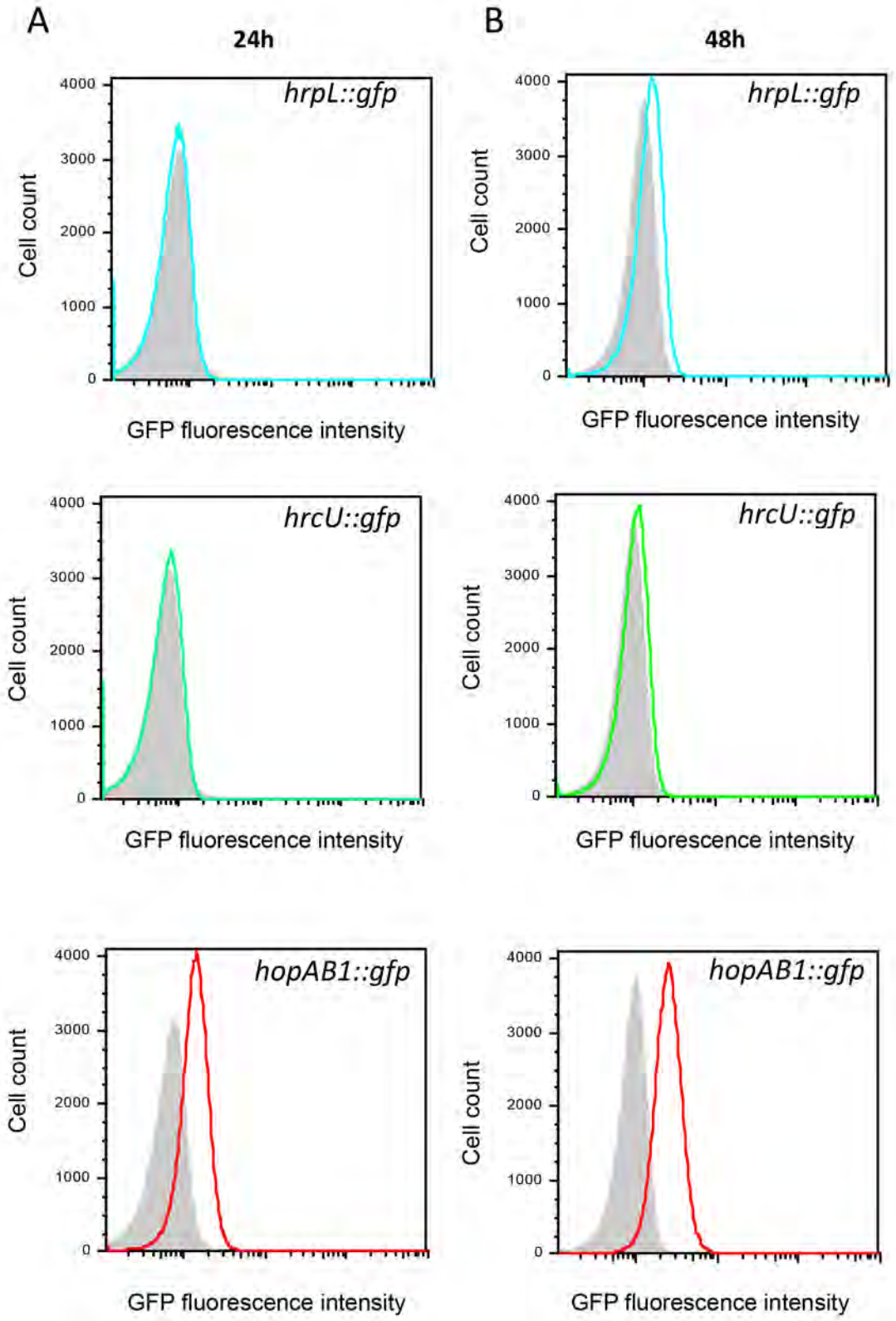
A
24h
B
48h
hrpL::gfp
hrcU::gfp
hopAB1::gfp
Cell count
GFP fluorescence intensity
0
1000
2000
3000
4000

Figure S1

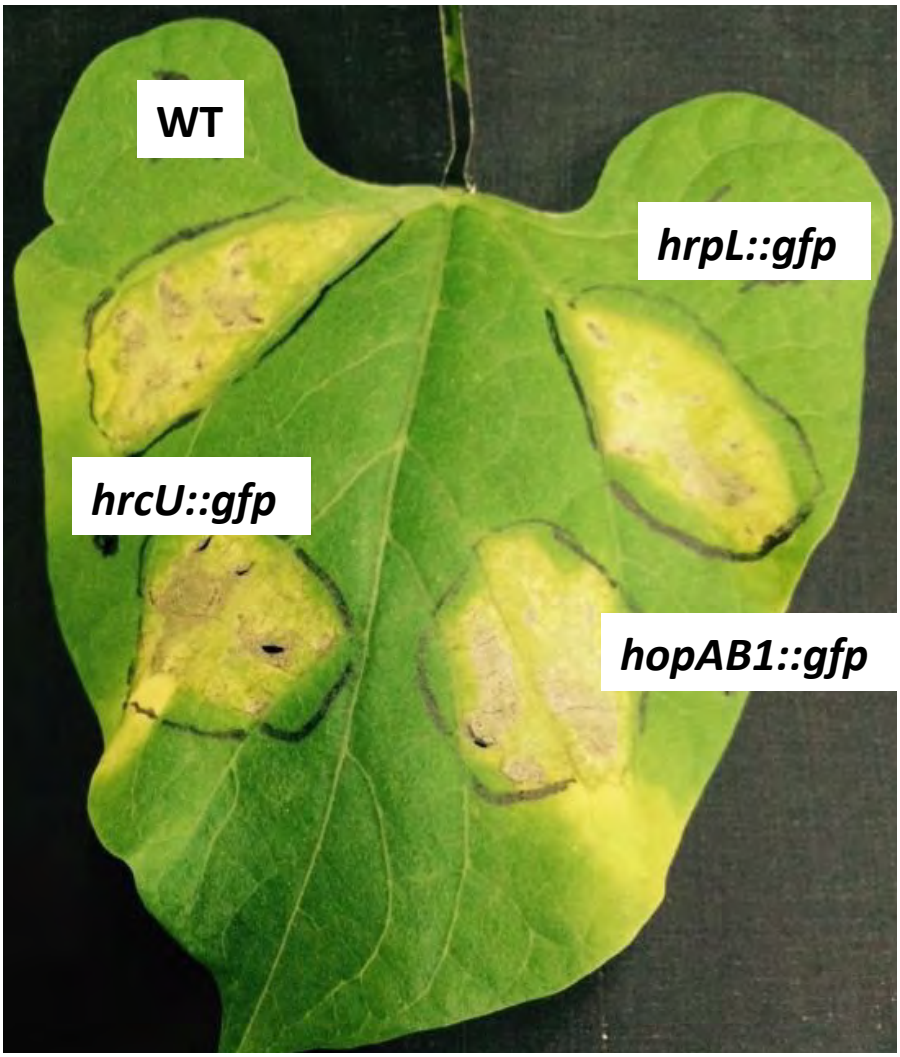

Fig S1. Strains carrying transcriptional fusions to gfp of hrpL, hrcU or hopAB1 display wild type virulence. Symptom development 7 days post inoculation of a bean leaf with $5x10^5$ cfu/ml or either wild type Pph 1448A or each of its derivatives carrying the indicated gene fusions.

Figure S3

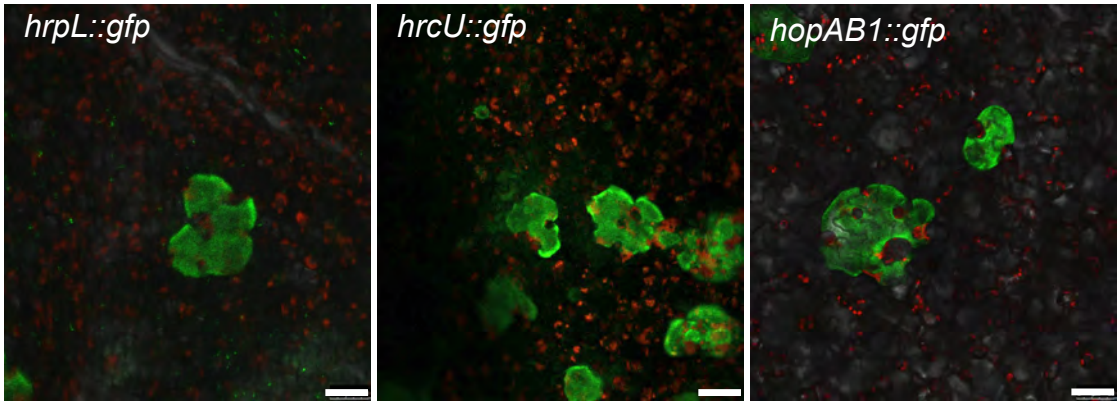

Fig S3. **Bacterial colonies display heterogeneous distribution of *gfp* fluorescence that cannot be unequivocally associated to individual cells.** Confocal microscopy images showing bacterial microcolonies within the apoplast of bean leaves, 5 days post-inoculation with $5x10^6$ cfu/ml of each of the strains carrying the chromosome-located transcriptional *hrpL::gfp, hrcU::gfp* or *hopAB1::gfp* fusions. Red corresponds to auto-fluorescence generated by chloroplasts. Scale bar corresponds to 50 µm.

Figure S4

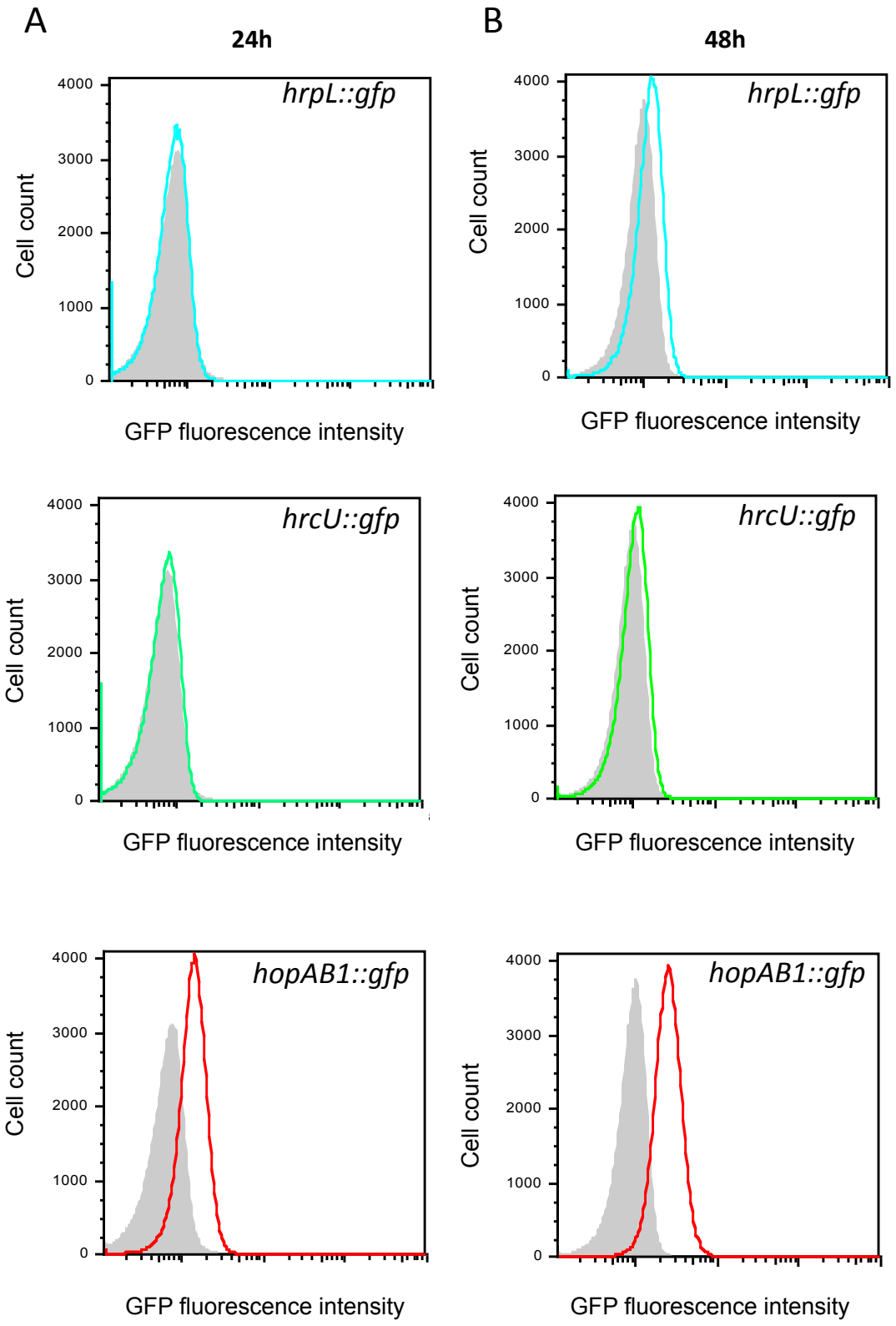

Figure S4. Flow cytometry analysis of in LB-grown bacterial cultures. Histograms of GFP fluorescence distribution in the strains carrying the chromosome-located transcriptional *hrpL::gfp, hrcU::gfp* or *hopAB1::gfp* fusions growing at 24h (**A**) or 48h (**B**). Grey histograms show a strain not expressing GFP. All data was collected for 100,000 events per sample.

Table 1. Strains used and generated in this work.

Strain	Genotype	Reference
1448A	*P. syringae* pv. *phaseolicola* wild-type strain race 6	Teverson, 1991
JRP9	1448A Tn*7*-eYFP, Gm^R	This work
JRP8	1448A Tn*7*-eGFP, Gm^R	This work
DLM1	1448A *hrpL::gpf,* Km^R	This work
DLM2	1448A *hrcU::gpf,* Km^R	This work
DLM3	1448A *hopAB1::gpf,* Km^R	This work
IOM49	1448A Δ*hrpA*	Ortiz-Martín et al., 2010a
JRP-F1	1448A Δ*hrpA; hrpL::gpf,* Km^R	This work
JRP-F2	1448A Δ*hrpA; hopAB1::gpf,* Km^R	This work
IOM57	1448A Δ*hrpG*	Ortiz-Martín et al., 2010b
IOM48-F	1448A Δ*hrpV*	Ortiz-Martín et al., 2010b
IOM58	1448A Δ*hrpG* Δ*hrpV*	Ortiz-Martín et al., 2010b
JRP-F3	1448A Δ*hrpG; hopAB1::gpf,* Km^R	This work
JRP-F4	1448A Δ*hrpV; hopAB1::gpf,* Km^R	This work
JRP-F5	1448A Δ*hrpG* Δ*hrpV; hopAB1::gpf,* Km^R	This work

Table 2. **Plasmids used in this work**.

Name	Description	Reference
pIOM22	pBBR1-MCS-4 derivative, contains a promotorless *hrpL* gene expressed from the *lacZ* promoter	Ortiz-Martín et al., 2010a
pIOM92	pBBR1-MCS-4 derivative, contains a promotorless *hrpG* gene expressed from the *lacZ* promoter	Ortiz-Martín et al., 2010b
pIOM53	pBBR1-MCS-4 derivative, contains a promotorless *hrpV* gene expressed from the *lacZ* promoter	Ortiz-Martín et al., 2010b

Table 3. **Primers used in this work**.

Name	Description	Restriction site
HrpL A1	CGGTATCCGTCAACTGACGG	NA
HrpL A2	GAATTCTATCCACTCAGGCGAACGGG	*Eco*RI
HrpL B1	TGAGTGGATAGAATTCTCTGTCTGGAACCAAC TCGC	*Eco*RI
HrpL B2	ATGGGCGACCATCGGATCC	NA
HrcU A1	GTGATTCTGGGGTTGCTGC	NA
HrcU A2	GAATTCAGCTCCCAGCTTAAAGCTCC	*Eco*RI
HrcU B1	AGCTGGGAGCTGAATTCGCAAGCCAGGCGTA ACAGG	*Eco*RI
HrcU B2	TTCTACTACAACGTCGCTGC	NA
HopAB1 A1	GCATCCTTTATAACTGACCC	NA
HopAB1 A2	GAATTCCTGAAATCAGTTCAGCTTAACG	*Eco*RI
HopAB1 B1	CTGATTTCAGGAATTCTCGTTGTAGTGGCCGG	E*co*RI
HopAB1 B2	GGACAGGTCGTAGTAGAGCG	NA
Zep07F	GAATTCTAAGAAGGAGATATACATATGAG	NA
Zep07F	GAATTCTTATCACTTATTCAGGCGTA	NA